Ultrahigh-capacity reversible hydrogen storage in BN-biphenylene under environmental conditions

Fengyu Miao,[1,*] Jie Li,[2,*,†] Lingzhi Wu,[3] Xin Huang,[3] Zhihong Yang,[3] Yunhui Wang,[3,‡] and Yakui Weng[3,4,§]

[1]*College of Electronic and Optical Engineering, Nanjing University of Posts and Telecommunications, Nanjing 210023, China*

[2]*Grünberg Research Centre, Nanjing University of Posts and Telecommunications, Nanjing 210023, China*

[3]*School of Science, Nanjing University of Posts and Telecommunications, Nanjing 210023, China*

[4]*Key Laboratory of Quantum Materials and Devices of Ministry of Education, School of Physics, Southeast University, Nanjing 211189, China*

(Received 31 January 2024; accepted 3 July 2024; published 18 July 2024)

Although the use of two-dimensional materials for hydrogen storage has been intensively studied, finding reversible hydrogen storage material with high hydrogen gravimetric density under environmental conditions remains challenging. In this study, a new two-dimensional BN-biphenylene with Li decoration is systematically investigated through density functional theory (DFT) and grand canonical Monte Carlo (GCMC) simulations. The DFT results reveal that the average binding energy between Li and BN-biphenylene monolayers can be significantly improved from −0.9 eV to −3.34 eV by doping two C atoms at N sites. In this sense, each Li atom can adsorb three H_2 molecules, yielding a high H_2 weight density of 12.54 wt%. Meanwhile, considering the corresponding H_2 desorption temperature at the ideal environmental condition of 323.89 K, Li-modified C-doped BN-biphenylene monolayer can be treated as a promising reversible candidate for high-density hydrogen storage. In addition, GCMC simulation results also prove that the H_2 storage capacity of Li-modified C-doped BN-biphenylene can reach an ultrahigh 13.28 wt% under 298 K and 1 bar. The present study provides a positive and valuable reference for exploring ultrahigh-capacity reversible hydrogen storage materials under environmental conditions.

DOI: 10.1103/PhysRevMaterials.8.075401

I. INTRODUCTION

Energy issues have always been of great concern. On one hand, the use of fossil fuels, such as coal and oil, has contributed to economic development, but on the other hand, the use of fossil fuels has indeed led to serious environmental pollution, including air and water pollution, as well as problems related to climate change [1,2]. Therefore, the search for environmentally friendly and efficient clean energy has become a hot research topic. Hydrogen, as a green and highly efficient secondary energy source, is considered to be an ideal candidate material for realizing carbon-free energy because of its numerous advantages, such as abundant resources, high calorific value and no harmful emissions [3]. Currently, the hydrogen storage target of gravimetric density set by the U.S. Department of Energy (DOE) is 5.5 wt% before 2025 [4,5]. Here, the 5.5 wt% value is the DOE target for the entire hydrogen storage system, not just for the active hydrogen storage material. Meanwhile, the average hydrogen adsorption energy should be in the range of $-0.2 \sim -0.6\,\mathrm{eV}/H_2$ to realize reversible hydrogen storage [6,7].

However, efficient storage and safe transportation of hydrogen remain challenges for the development of hydrogen economy [8]. Traditional hydrogen storage methods, such as high-pressure gasification and low-temperature liquefaction, require extremely stringent safety measures and are often accompanied by heavy energy consumption and serious evaporation losses, severely limiting the development and application of hydrogen energy [9,10]. On the contrary, solid-state physical storage, where hydrogen is physically adsorbed onto the surface of a material for storage and release [11], is expected to be the major method of hydrogen storage in the future, as it can meet the safety, reversibility, and high efficiency that are urgently needed for hydrogen energy applications.

In general, stable and efficient physical hydrogen storage primarily involves two key steps: (i) selection of suitable substrate materials and (ii) enhancement of hydrogen storage capacity by metal modification, strain effect, and doping effect. Over the past few years, most previous works on hydrogen storage were based on the carbon-based two-dimensional (2D) materials, such as graphdiyne [12], graphyne [13], and Irida-graphene [14], because of their excellent properties of large specific surface area, exceptional chemical stability, and light weight. However, carbon-based materials are highly susceptible to oxidation or even combustion at high temperature [15], which is not conducive to the practical application of hydrogen storage. Recently, some studies have shown that B-N-based 2D materials are more advantageous for hydrogen storage than carbon-based counterparts [16,17]. First, B-N-based 2D materials possess superior thermal stability and are more suitable for hydrogen storage at ambient temperatures [18]. Second, pure B-N-based 2D materials have better hydrogen storage capacity than pure carbon-based materials with the same geometrical configuration [19,20]. Therefore,

*These authors contributed equally to this work.
†Contact author: lijie@njupt.edu.cn
‡Contact author: yhwang@njupt.edu.cn
§Contact author: wyk@njupt.edu.cn

B-N-based 2D materials may be promising candidates for high-performance hydrogen storage.

To improve the binding energy between H_2 and 2D materials, the metal decoration strategy is usually used as the first option [21,22], which can construct an effective internal electric field. Among all metal atoms, the alkali metal Li is often used as the first candidate for metal modification because its lightest atomic mass allows for the highest storage mass ratio to some extent. For example, Paramita *et al.* found that the average H_2 adsorption energy of Li-decorated hydrogenated h-BN nanosheet can reach a desirable range of -0.18 to -0.3 eV/H_2 [23]. Yong *et al.* reported that 12.31 wt% of the hydrogen storage mass ratio can be achieved for Li-modified T-BN [24]. Nevertheless, for some 2D systems modified by metal atoms, a natural but obligatory problem, i.e., the phenomenon of metal clustering on the substrate surface, will be frequently encountered. For example, the binding energies of Li on B_6N_6 and BN fullerene are 0.80 eV and 0.725 eV, respectively [25,26], both of which are smaller than the cohesion energy of Li (1.63 eV), implying the easy formation of Li clusters. To avoid metal-clustering behavior on the surface of 2D materials and improve the hydrogen storage capacity, doping methods are often preferred because their remarkable effects have been repeatedly demonstrated [27]. For example, for Li-modified phagraphene, the binding energy after doping B atoms is 0.8 eV higher than that of the undoped structure, and the corresponding hydrogen storage capacity reaches 13.07 wt% [28]. Similarly, for Li-modified biphenylene, doping with N atoms increased the storage density from 9.58 wt% to 10.59 wt% [29].

Recently, Ma *et al.* theoretically predicted a new stable 2D B-N counterpart of biphenylene structure (bi-BN) consisting of 4-, 6-, and 8-membered rings [30]. Its excellent structural stability and unique symmetric voids are very favorable for metal modification and atomic doping, and thus may exhibit high-performance hydrogen storage behavior. In this study, using density-functional theory (DFT) and grand canonical Monte Carlo (GCMC) simulation methods, the hydrogen adsorption/release capacity of Li-modified 2D bi-BN material has been investigated systematically. To prevent Li atoms clustering and further enhance the binding energy between Li and bi-BN monolayer, carbon atoms are introduced to the bi-BN structure. The DFT results reveal that the hydrogen storage weight ratio of Li-modified C-doped bi-BN can reach 12.54 wt% with ideal H_2 desorption temperature (T_D) of ~323.89 K. In addition, according to the GCMC simulations, the hydrogen storage capacity of Li-modified C-doped bi-BN can reach an ultrahigh 13.28 wt% under 298 K and 1 bar (environmental conditions). These findings will further enrich the application of BN-based 2D materials in hydrogen storage and encourage more theoretical and experimental studies to explore the high-performance of bi-BN materials for reversible hydrogen storage under environmental conditions.

II. METHODS

The structural optimization and electronic property calculations were performed using the Vienna *ab initio* simulation package (VASP) code based on the generalized gradient approximation (GGA) with Perdew-Burke-Ernzerhof (PBE) potentials [31,32]. For the 2D bi-BN monolayer, a vacuum space of 25 Å along the *c*-axis direction was introduced to avoid layer interactions. The cutoff energy of the plane wave was fixed to 550 eV. Monkhorst-Pack *k*-point meshes of $9 \times 7 \times 1$ and $11 \times 9 \times 1$ centered at the Γ point were adopted for structural optimization and static calculations, respectively. To better describe the van der Waals (vdW) interaction during hydrogen adsorption, the correction DFT-D2 method of Grimme is applied [33]. The energy convergence criterion was set to be 1×10^{-6} eV. The in-plane lattice constants and atomic positions were fully optimized until the force on each atom was less than 0.01 eV/Å.

To illustrate the interactions within the system, CP2K program package was employed to optimize the structure after H_2 adsorption and output the wavefunction (molden) files [34]. Then, the Multiwfn program [35] was used to analyze the molden files and generate an independent gradient model based on Hirschfeld partitioning (IGMH) [36]. At last, the visualization of system interactions through the IGMH method can be achieved by using the VMD software package [37].

To test the structural stability at room temperature (i.e., ~300 K), the *ab initio* molecular dynamics (AIMD) simulations were carried out under NVT conditions (where N, V, and T represent particle number, system volume, and system temperature, respectively) [38]. The total simulation time was 10 ps with a time step of 1 fs. In addition, to verify and further enrich the results of DFT, GCMC simulations of hydrogen adsorption were performed using the Dreiding force field with 5 000 000 steps for both equilibrium and production [39–41].

In this work, the average binding energy (E_b) between Li atoms and the bi-BN substrate can be written as

$$E_b = (E_{m\text{Li-substrate}} - mE_{\text{Li}} - E_{\text{substrate}})/m, \quad (1)$$

where m represents the number of Li atoms. $E_{m\text{Li-substrate}}$, E_{Li}, and $E_{\text{substrate}}$ are the energies of the Li-modified substrate, the Li atom, and the substrate, respectively. The average adsorption energy (E_{ads}) and consecutive adsorption energy (E_c) of hydrogen molecules can be obtained using the following equations:

$$E_{ads} = (E_{n\text{H2-}m\text{Li-substrate}} - nE_{\text{H2}} - E_{\text{substrate}})/n, \quad (2)$$

$$E_c = (E_{n\text{H2-}m\text{Li-substrate}} - E_{(n\text{-}2)\text{H2-}m\text{Li-substrate}} - 2E_{\text{H2}})/2, \quad (3)$$

where n represents the number of H_2 molecules. $E_{n\text{H2-}m\text{Li-substrate}}$, $E_{(n-2)\text{H2-}m\text{Li-substrate}}$, and E_{H2} are the energies of Li-modified substrate with n H_2 molecules, Li-modified substrate with n-2 H_2 molecules, and one H_2 molecule, respectively. The H_2 gravimetric percentage (G) can be obtained based on the following equation:

$$G(wt\%) = nM_{\text{H2}}/(nM_{\text{H2}} + M_{m\text{Li-substrate}}), \quad (4)$$

where M_{H2} and $M_{m\text{Li-substrate}}$ are the total mass of H_2 and the Li-modified substrate, respectively.

III. RESULTS AND DISCUSSION

The optimized structure of pure bi-BN monolayer is shown in Fig. 1(a), which includes 12 B atoms and 12 N atoms. It can be clearly seen that all B and N atoms remain in the same plane without folding, qualitatively indicating the structural

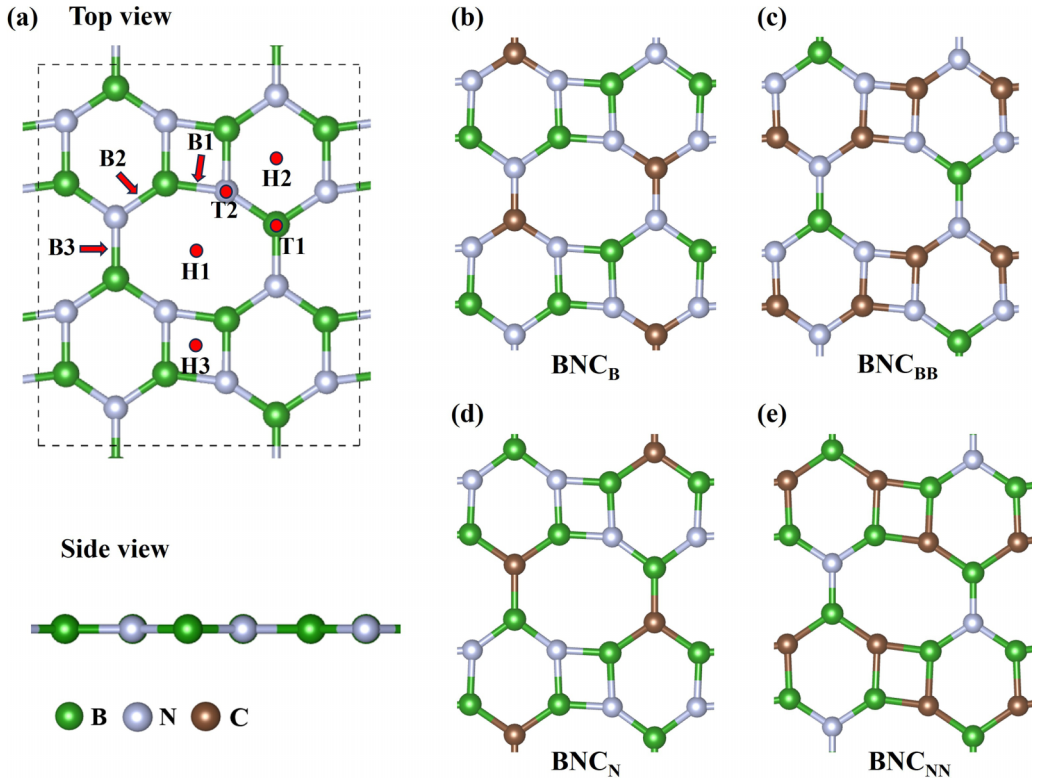

FIG. 1. (a) Top and side views for the optimized structure of pure BN-biphenylene. The possible adsorption sites, including three hollow sites (H1, H2, H3), three bridge sites (B1, B2, B3), and two top sites (T1, T2), are indicated. (b) One B atom is replaced by one C atom in a six-membered ring, defined as BNC_B. (c) Two B atoms replaced by two individual C atoms in a six-membered ring, defined as BNC_{BB}. (d) One N atom replaced by one C atom in a six-membered ring, defined as BNC_N. (e) Two N atoms replaced by two individual C atoms in a six-membered ring, defined as BNC_{NN}.

stability of the bi-BN monolayer. The optimized structure gives $a = 7.656$ Å and $b = 9.091$ Å, which are consistent with the results of previous studies [42,43].

As the first step, the hydrogen storage performance of pure bi-BN monolayer is studied. Here, the adsorption energy of individual H_2 molecules on various adsorption positions of bi-BN substrate [including the hollow sites of the eight-, six-, and four-membered rings: H1, H2, and H3; The top sites of three different B-N bonds: B1, B2, and B3; the top sites of B and N atoms: T1 and T2, see Fig. 1(a)] was checked and compared. According to our calculation, the H_2 molecule adsorbed at the H2 site (i.e., the hollow site of the six-membered ring) of bi-BN substrate is the most stable state. The corresponding distance between the H_2 molecule and the bi-BN substrate is 2.79 Å, yielding a small adsorption energy of $-0.09\,eV/H_2$, which is far from the practical application criterion of H_2 adsorption.

To increase H_2 adsorption energy, Li atom modification is considered. Clearly, there are three most likely metal adsorption sites on bi-BN monolayer, i.e., H1, H2, and H3. However, the calculated binding energies of these three sites are -0.94 eV, -0.91 eV, and -0.72 eV, respectively, which are all less than the cohesive energy of bulk Li (1.63 eV), suggesting that Li atoms are very likely to form clusters on the BN surface. To avoid this scenario, doping effect is performed. Here, we introduce carbon (C) atoms into the bi-BN monolayer to enhance the binding energy.

As shown in Figs. 1(b)–1(e), the sites and proportions of C doping in the bi-BN monolayer have been investigated. Focusing on the B_3N_3 six-membered ring, there are four possible doping modes: (1) one B atom replaced by one C atom (defined as BNC_B); (2) two B atoms replaced by two individual C atoms (defined as BNC_{BB}); (3) one N atom replaced by one C atom (defined as BNC_N); (4) two N atoms replaced by two individual C atoms (defined as BNC_{NN}). Here, to obtain the highest hydrogen storage capacity, double-side Li atoms modified symmetrically at the H2 site of the C-doped bi-BN monolayer are employed. The calculated average binding energies of Li atoms on BNC_B, BNC_{BB}, BNC_N, and BNC_{NN} are -1.22 eV, -1.16 eV, -2.83 eV, and -3.34 eV, respectively (details about adsorption structures can be found in Fig. 2(a) and the Supplemental Material [44]). By comparing these values, it can be seen that the structure with C atoms instead of N atoms (i.e., BNC_N and BNC_{NN}) is more stable than the structure with C atoms instead of B atoms (i.e., BNC_B and BNC_{BB}). The physical mechanism is that replacing N atoms with C atoms will introduce electron vacancies, thereby more significantly increasing the charge transfer and interaction between Li and the substrate. As shown in Fig. 2(c) and Fig. S1 [44], more charges are obviously gathered around C than around N and B. In this sense, Li-modified BNC_{NN} structure [including 8 Li, 12 B, 8 C, and 4 N atoms, see Fig. 2(a)] is more suitable as a hydrogen storage substrate than the other three doping structures, and is

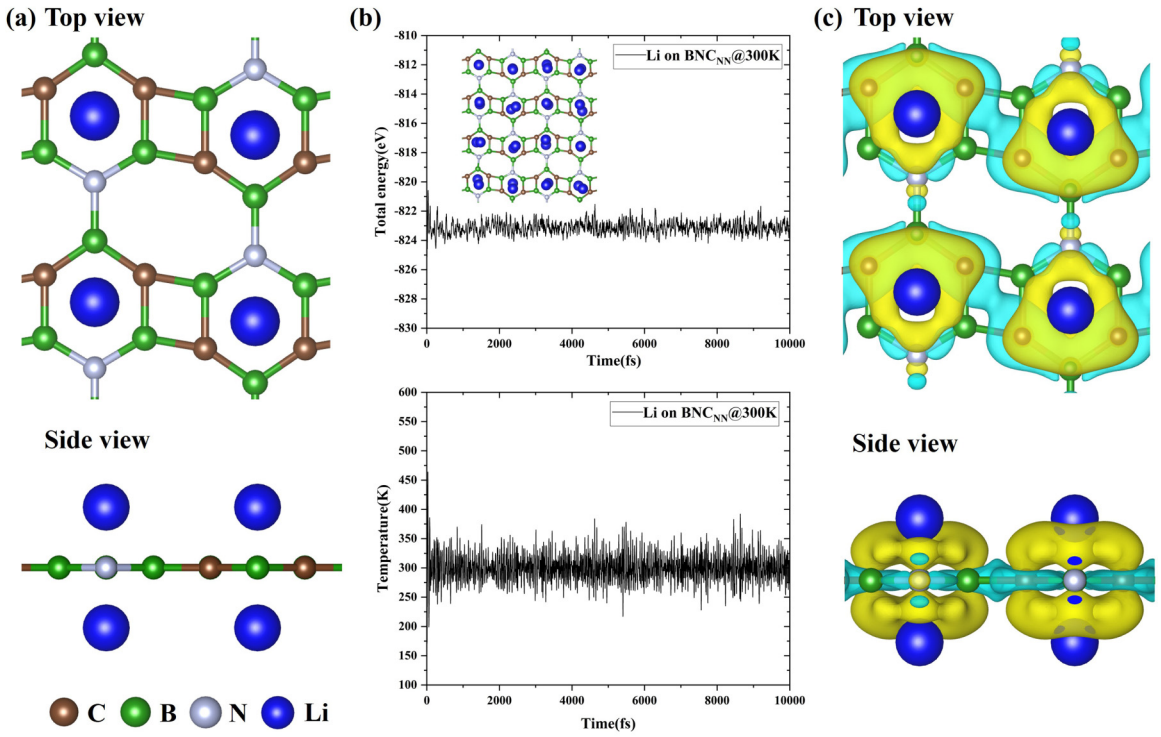

FIG. 2. (a) Top and side views of optimized Li-decorated BNC_{NN} monolayer. (b) Fluctuations of the total energy and temperature as a function of simulation time for Li-decorated BNC_{NN} at 300 K by using AIMD simulations. (c) Top and side views of charge density differences for Li-decorated BNC_{NN} monolayer. Yellow and cyan represent charge accumulation and depletion, respectively.

therefore adopted as the default structure in the following calculations.

Before discussing the hydrogen storage performance of Li-modified BNC_{NN} monolayer, it is necessary to check the structural stability. As shown in Fig. 2(b), AIMD simulations were performed at room temperature of 300 K. It can be seen that the energy and temperature fluctuated little throughout the 10 ps simulation, and no significant metal displacement as well as structural breakage was observed, indicating that the Li-modified BNC_{NN} structure is thermodynamically stable. In fact, such structural stability can also be qualitatively confirmed by the charge density difference $\Delta\rho$ (defined as $\Delta\rho = \rho_{\text{Li-substrate}} - \rho_{\text{Li}} - \rho_{\text{substrate}}$, where $\rho_{\text{Li-substrate}}$, ρ_{Li}, and $\rho_{\text{substrate}}$ are the charge densities of the Li-modified substrate, the Li atoms, and the substrate, respectively), the projected density of state (PDOS), and Bader charge. As shown in Fig. 2(c) and Fig. S1(a) [44], the amount of charge transferred from Li to the BNC_{NN} is significantly more than that transferred from Li to the pure BN, implying that C doping effectively strengthens the interaction between Li and the substrate, in agreement with previous studies [45]. Such increased charge transfer can also be analyzed from the Bader charge. As listed in Table S1 [44], the number of transferred electrons between Li and the substrate increased from 0.644 e^-/atom to 0.823 e^-/atom after C doping. In addition, the high overlap between C and BN (as well as between Li and the substrate) over a wide energy range implies strong orbital hybridization among these atoms (see Fig. S2 [44]), which ensures the stability of the structure and avoids the clustering of Li atoms.

Then, the hydrogen storage performance of Li-modified BNC_{NN} monolayer has been investigated in detail. In our calculated unit cell, a total of 8 Li atoms are used for modification on both sides of the substrate, and H_2 molecules are introduced into the system one by one. The optimized structures with different numbers of H_2 molecule adsorption are sketched in Fig. 3. In general, the adsorption site of the first H_2 molecule is crucial because it largely determines the position of subsequent H_2 molecules and the maximum hydrogen storage capacity of the material. Here, we try to place the first H_2 molecule on top of B atom, C atom, N atom, and B-C bonds, respectively. The structural optimization shows that the first H_2 molecule preferentially occupies the adsorption site near the top of the C atom and tilts toward the metal Li atom [see Fig. 3(a)], which can be understood from the strength distribution of the internal electric field. In this Li-modified BNC_{NN} structure, the charge accumulation and depletion between Li and C atoms are significantly more than that between Li and B atoms as well as between Li and N atoms [see Fig. 2(c)], leading to a stronger vertically oriented internal electric field, which makes the H_2 molecules more willing to adsorb near the top of the C atoms. The corresponding adsorption energy of H_2 is -0.33 eV/H_2 (see Table I), which is much higher than that of the system without Li modification (~ -0.08 eV/H_2, see Fig. S3 [44]), confirming once again that Li modification is very effective in enhancing the hydrogen storage capacity. Meanwhile, the bond length of H-H ($d_{\text{H-H}}$) increases slightly from 0.740 Å in the isolated state to 0.774 Å in the adsorbed state due to the adsorption of Li-modified substrate.

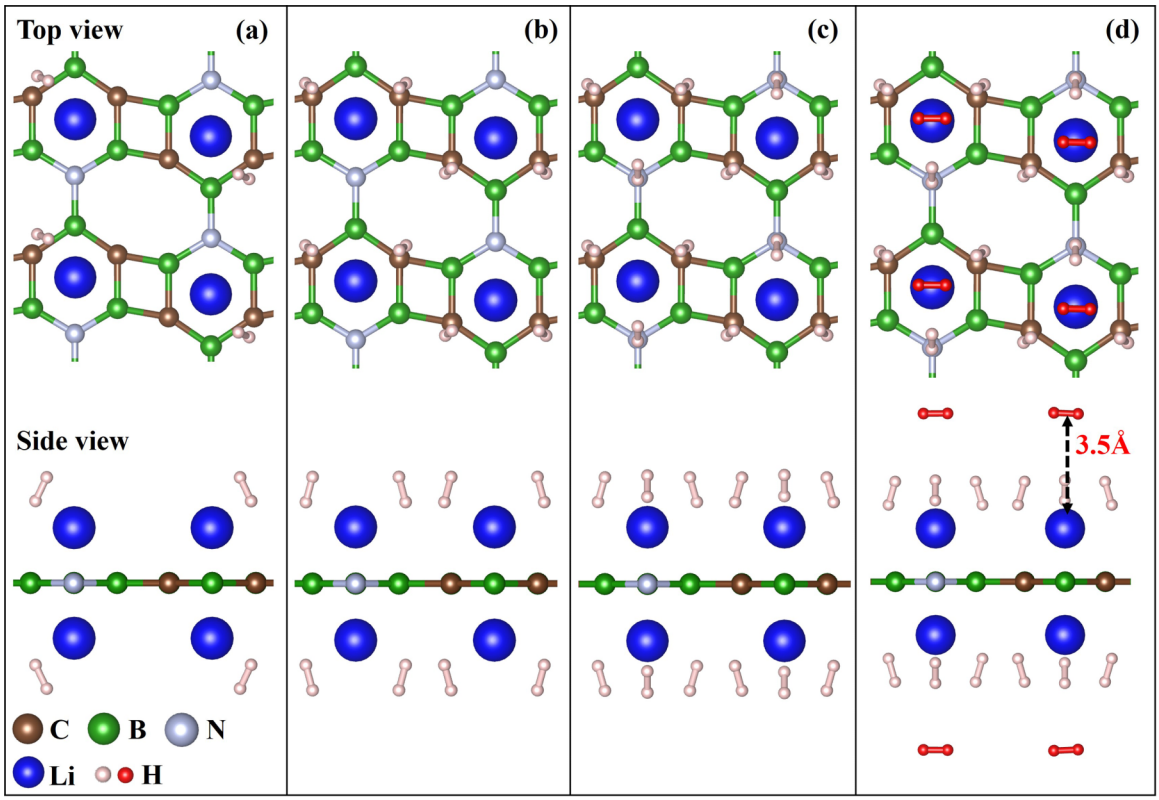

FIG. 3. The optimized structures of (a) $8H_2$ ($1H_2$ per Li), (b) $16H_2$ ($2H_2$ per Li), (c) $24H_2$ ($3H_2$ per Li), and (d) $32H_2$ ($4H_2$ per Li) adsorbed on Li-decorated BNC_{NN} monolayer.

Next, the second, third, and fourth H_2 molecules are sequentially placed into the system. As shown in Figs. 3(b)–3(d), the detailed adsorption positions are as follows: the second H_2 molecule is symmetrically attached to the top of another C atom in the six-membered ring; the third H_2 molecule is adsorbed on top of the N atom, forming a planar triangular structure with the previous two H_2 molecules. However, when the fourth H_2 molecule is initially placed in the same plane as the previous three H_2 molecules, its position would be optimized above the Li atom, suggesting that the previously mentioned planar space may be too narrow to store the fourth H_2 molecule. In this sense, the fourth H_2 molecule placed directly above the Li atom is considered, and the optimized structure is shown in Fig. 3(d).

We now move our attention to the calculation data, which include the average distance $d_{\text{Li-substrate}}$ between Li and the substrate, average distance $d_{\text{Li-H2}}$ between Li and H_2 molecule, bond length $d_{\text{H-H}}$ of H-H, and average (or consecutive) adsorption energy E_{ads} (or E_c). As summarized in Table I, in terms of the average properties of H_2 adsorption, as the number of H_2 molecules increases (from $1H_2$/Li to $4H_2$/Li), the distance between Li and H_2 molecules gradually increases from 1.913 Å to 2.394 Å, while the average adsorption energy (E_{ads}) decreases from $-0.33\,\text{eV}/H_2$ to $-0.21\,\text{eV}/H_2$, which is still in the effective range (-0.2 eV to $-0.6\,\text{eV}/H_2$) for stable hydrogen storage. Meanwhile, the value of $d_{\text{H-H}}$ is always around 0.76 Å, indicating that H_2 molecules are indeed gathered around Li atoms through physical adsorption, which is beneficial for the rapid release of H_2 molecules.

However, when we focus on the adsorption of each H_2 molecule independently, it is found that when the number of adsorbed H_2 molecules increases from three to four, the corresponding distance between Li and the fourth H_2 molecule increased dramatically to 3.5 Å [see Fig. 3(d)], resulting in the consecutive adsorption energy (E_c) of H_2 molecules undergoing an abrupt decrease from -0.20 eV to -0.07 eV (see Table I). The underlying mechanism is that in the process of physical adsorption, the H_2 adsorption is mainly based on

TABLE I. The average distance between Li and H_2 molecules ($d_{\text{Li-H2}}$), the average H-H bond length ($d_{\text{H-H}}$), the average adsorption energy per H_2 (E_{ads}), the consecutive adsorption energy (E_c), the desorption temperature (T_D), and the corresponding hydrogen storage capacity.

Systems	n	$d_{\text{Li-H2}}/d_{\text{H-H}}$(Å)	E_{ads} (eV)	E_c (eV)	T_D	Gravimetric density
8Li-BNC_{NN}	$8H_2$	1.913/0.774	−0.33	−0.33	422.89	4.56 wt%
	$16H_2$	1.984/0.768	−0.28	−0.23	355.99	8.73 wt%
	$24H_2$	1.992/0.764	−0.25	−0.20	323.89	12.54 wt%
	$32H_2$	2.394/0.758	−0.21	−0.07	256.61	16.05 wt%

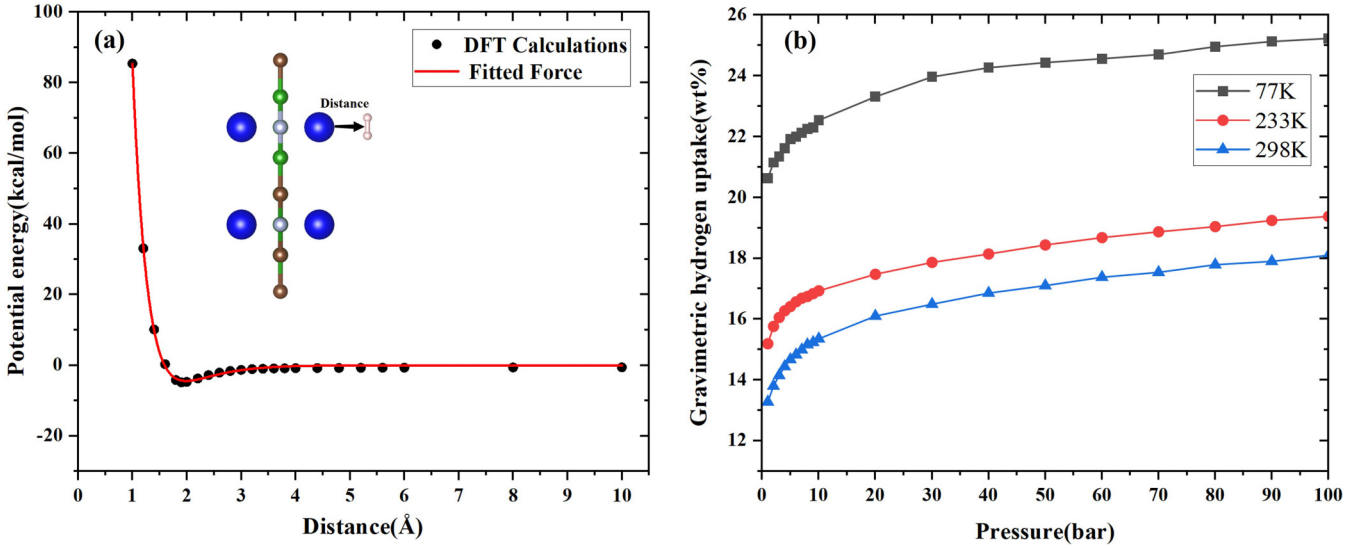

FIG. 4. (a) Comparison of the DFT calculations and fitted force field between H_2 and Li-decorated BNC_{NN}. (b) Calculated H_2 adsorption gravimetric for Li decorated BNC_{NN} at 77 K, 233 K, and 298 K with the pressure ranged from 1 bar to 100 bar.

the internal electric field between Li atoms and the substrate (see polarized H_2 molecules and weak orbital hybridization in Fig. S4 [44]). Once the distance between the H_2 molecule and Li atom exceeds a certain limit, the H_2 molecule can easily diffuse away under thermal perturbation, thus leading to a substantial decrease in adsorption energy. According to previous studies, both the $d_{Li\text{-}H2}$ greater than 2.5 Å and E_c less than 0.1 eV imply that H_2 adsorption is ineffective [46,47]. Therefore, the 8Li-modified BNC_{NN} monolayer adsorbed with 24 H_2 molecules is considered to be the most reasonable hydrogen storage system, and its thermodynamic stability has been confirmed by AIMD. As shown in Fig. S5 [44], the fluctuations in temperature and total energy over time are within reasonable ranges, indicating that the Li-modified BNC_{NN} monolayer with the presence of H_2 is thermodynamically stable. In addition, all the Li atoms are independently located in the six-membered ring and no aggregation occurs. Therefore, the H_2 adsorption has no obvious effect on the stability of Li-modified BNC_{NN} monolayer and does not lead to the aggregation of Li atoms.

Meanwhile, it is necessary to consider whether Li-modified BNC_{NN} monolayer with H_2 is capable of forming LiH or LiC compounds. Here, the IGMH method is employed to illustrate the interaction between Li and BNC_{NN} monolayers (as well as between H_2 molecules and the Li-modified substrate). First, Li atoms are denoted as fragment 1, while the BNC_{NN} monolayer is referred to as fragment 2. As shown in Figs. S6(a) and S6(b) [44], the primary mode of interaction between Li and BNC_{NN} monolayers is through van der Waals forces, which do not meet the bonding criteria of LiC compounds. Then, the H_2 molecules are denoted as fragment 1, while the Li-modified BNC_{NN} monolayer is referred to as fragment 2. Similarly, the primary mode of interaction between H_2 molecules and Li is through van der Waals forces [see Figs. S6(c) and S6(d) [44]], in agreement with a previous study [48], which again do not satisfy the bonding criteria of LiH compounds. Therefore, the formation of LiH or LiC compounds can be excluded in this system. Moreover, the overall structural stability at a very high temperature of 600 K is tested by using AIMD simulations. As shown in Fig. S7 [44], all the hydrogen still exists in the form of H_2 molecules instead of H atoms, implying that H_2 molecules are difficult to dissociate on the Li-modified BNC_{NN} monolayer.

As summarized in Table I, the hydrogen storage capacity of Li-modified BNC_{NN} monolayer is 12.54 wt%. The corresponding desorption temperature (T_D) reaches the ideal environmental temperature of ~323.89 K, which is favorable for the practical application of hydrogen storage [49,50]. To present the hydrogen storage capacity of Li-modified BNC_{NN} more intuitively, we compared it with other Li-modified B-N-C 2D materials [51–55]. As shown in Table S3 [44], the Li-modified BNC_{NN} monolayer has both ultrahigh hydrogen storage capacity and excellent desorption temperature. Such an excellent desorption temperature indicates that storage does not need to cost much (such as high-pressure hydrogen storage) for on-board applications, which need further experimental confirmation and verification. These results indicate that Li-modified BNC_{NN} monolayer can serve as very promising high-capacity reversible hydrogen storage material for future hydrogen energy economy.

At last, considering the actual conditions of hydrogen storage, GCMC simulation is used to calculate the hydrogen storage capacity of Li-decorated BNC_{NN} at different temperature and pressure conditions. First, the Dreiding force field parameters are obtained by fitting the DFT results with the Morse equation [56], as listed in Table S2 [44]. The corresponding Morse potential energy curve is shown in Fig. 4(a). It can be seen that an obvious potential energy well appears at a distance close to 2 Å between Li and H_2 molecules, indicating that this distance is the optimal location for H_2 molecule adsorption. Then, based on the parameters fitted above, the isotherms of H_2 molecules on Li-modified BNC_{NN} at 77 K, 233 K, and 298 K are calculated as a function of pressure. As shown in Fig. 4(b), under 298 K (room temperature) and 1 bar, the hydrogen storage capacity is 13.28 wt%. As the pressure increases, the hydrogen storage capacity rises rapidly, even

reaching an impressive 18.10 wt% at 100 bar. In addition, the lower the temperature, the higher the hydrogen storage capacity. Under 1 bar, the hydrogen storage weight ratios at 233 K and 77 K are 15.19 wt% and 20.63 wt%, respectively. When the pressure is increased to 100 bar, the hydrogen storage weight ratios at 233 K and 77 K increase to 19.38 wt% and 25.23 wt%, respectively. Therefore, combining the ideal desorption temperature (i.e., ∼323.89 K) discussed above and the high hydrogen storage weight ratios under ambient conditions, Li-modified BNC_{NN} can be treated as a very promising material for reversible hydrogen storage.

IV. CONCLUSION

In summary, the hydrogen storage performance of Li-modified C-doped BN-biphenylene has been investigated using first-principles calculations and GCMC simulations. Initially, the very weak adsorption energy ($-0.09\,eV/H_2$) of H_2 molecules on pure BN-biphenylene prompted us to adopt the method of Li modification. However, Li atoms tend to form clusters on the surface of pure BN-biphenylene due to the small binding energy (−0.9 eV). To avoid this scenario, C doping effect is employed to enhance the charge transfer as well as the binding energy between the Li atom and the substrate. It is found that the structure with C atoms instead of N atoms is most stable with high energy of −3.34 eV. According to the successive adsorption energy of H_2, each Li atom can physically adsorb three H_2 molecules with an average adsorption energy of $-0.25\,eV/H_2$. Then, a total of 24 H_2 molecules can be adsorbed by the double-sided 8Li-decorated C-doped BN-biphenylene monolayer, corresponding to a hydrogen gravimetric capacity of 12.54 wt%. In addition, such the thermodynamic stability of the saturated hydrogen storage structure at 300 K has been confirmed by molecular dynamics simulations. Considering the hydrogen desorption temperature under ideal environmental condition of ∼323.89 K, the Li-modified C-doped BN-biphenylene monolayer can be treated as a promising reversible candidate for high-density hydrogen storage. Furthermore, GCMC results also prove that the H_2 storage capacity of Li-modified C-doped BN-biphenylene can reach an ultrahigh 13.28 wt% under 298 K and 1 bar, realizing ultrahigh-capacity reversible hydrogen storage under environmental conditions. Further experimental and theoretical studies are expected to confirm and expand these predictions.

ACKNOWLEDGMENTS

This work was supported by the Natural Science Foundation of Nanjing University of Posts and Telecommunications (Grant No. NY222167) and the open research fund of Key Laboratory of Quantum Materials and Devices (Southeast University), Ministry of Education.

The authors declare that they have no known competing financial interests or personal relationships that could have appeared to influence the work reported in this paper.

[1] J. O. Abe, A. P. I. Popoola, E. Ajenifuja, and O. M. Popoola, Int. J. Hydrogen Energy **44**, 15072 (2019).
[2] C.-J. Winter, Int. J. Hydrogen Energy **34**, S1 (2009).
[3] V. R. Coluci, S. F. Braga, R. H. Baughman, and D. S. Galvão, Phys. Rev. B **75**, 125404 (2007).
[4] L. E. Klebanoff and J. O. Keller, Int. J. Hydrogen Energy **38**, 4533 (2013).
[5] U.S. Department of Energy, Available from: https://www.energy.gov/eere/fuelcells/doe-technical-targets-onboardhydrogen-storage-light-duty-vehicles.
[6] Y. H. Kim, Y. Zhao, A. Williamson, M. J. Heben, and S. B. Zhang, Phys. Rev. Lett. **96**, 016102 (2006).
[7] Z. M. Ao and F. M. Peeters, Phys. Rev. B **81**, 205406 (2010).
[8] M. A. Rosen and S. Koohi-Fayegh, Energy Environ. Sci. **1**, 10 (2016).
[9] M. Aasadnia and M. Mehrpooya, Appl. Energy **212**, 57 (2018).
[10] J. Chen, S. Lin, M. Xu, F. Wang, Y. Shao, J. Hao, and Y. Li, ACS Materials Lett. **4**, 1402 (2022).
[11] U. Eberle, M. Felderhoff, and F. Schuth, Angew. Chem. Int. Ed. **48**, 6608 (2009).
[12] Y. Wang, G. Xu, S. Deng, Q. Wu, Z. Meng, X. Huang, L. Bi, Z. Yang, and R. Lu, Appl. Surf. Sci. **509**, 144855 (2020).
[13] Y. Wang, Q. Wu, S. Deng, R. Ma, X. Huang, L. Bi, and Z. Yang, Appl. Surf. Sci. **495**, 143621 (2019).
[14] Y.-F. Zhang and J. X. Guo, Int. J. Hydrogen Energy **50**, 1004 (2024).
[15] Q. M. Deng, L. Zhao, Y. H. Luo, M. Zhang, L. X. Zhao, and Y. Zhao, Nanoscale **3**, 4824 (2011).
[16] L. P. Zhang, P. Wu, and M. B. Sullivan, J. Phys. Chem. C **115**, 4289 (2011).
[17] J. S. Wang, C. H. Lee, and Y. H. Yap, Nanoscale **2**, 2028 (2010).
[18] Q. Cai, S. Mateti, H. Jiang, L. H. Li, S. Huang, and Y. Chen, Mater. Today Phys. **22**, 100575 (2022).
[19] L. P. Ma, Z. S. Wu, J. Li, E. D. Wu, W. C. Ren, and H. M. Cheng, Int. J. Hydrogen Energy **34**, 2329 (2009).
[20] P. Fu, J. Wang, R. Jia, S. Bibi, R. I. Eglitis, and H. X. Zhang, Comput. Mater. Sci. **139**, 335 (2017).
[21] W. Q. Deng, X. Xu, and W. A. Goddard, Phys. Rev. Lett. **92**, 166103 (2004).
[22] Y. Wang, Q. Wu, J. Mao, S. Deng, R. Ma, J. Shi, J. Ge, X. Huang, L. Bi, J. Yin, S. Ren, G. Yan, and Z. Yang, Appl. Surf. Sci. **494**, 763 (2019).
[23] P. Banerjee, B. Pathak, R. Ahuja, and G. P. Das, Int. J. Hydrogen Energy **41**, 14437 (2016).
[24] Y. Yong, Q. Hou, X. Yuan, H. Cui, X. Li, and X. Li, J. Energy Storage **72**, 108169 (2023).
[25] Y. Xu, Y. Zhang, F. Zhang, X. Huang, L. Bi, J. Yin, G. Yan, H. Zhao, J. Hu, Z. Yang, and Y. Wang, Int. J. Hydrogen Energy **50**, 475 (2023).
[26] N. S. Venkataramanan, R. V. Belosludov, R. Note, H. Mizuseki R.Sahara, and Y. Kawazoe, Chem. Phys. **377**, 54 (2010).
[27] J. Li, Y. Chen, N. Gong, X. Huang, Z. Yang, and Y. Weng, Chin. Phys. B **33**, 017502 (2024).

[28] X. Bi, F. Zhang, W. Chen, X. Huang, G. Yan, H. Zhao, Z. Yang, and Y. Wang, Appl. Surf. Sci. **638**, 157950 (2023).
[29] X. Zhang, F. Chen, B. Jia, Z. Guo, J. Hao, S. Gao, G. Wu, L. Gao, and P. Lu, Int. J. Hydrogen Energy **48**, 17216 (2023).
[30] X.-D. Ma, Z.-W. Tian, R. Jia, and F.-Q. Bai, Appl. Surf. Sci. **598**, 153674 (2022).
[31] G. Kresse and D. Joubert, Phys. Rev. B **59**, 1758 (1999).
[32] J. P. Perdew, A. Ruzsinszky, G. I. Csonka, O. A. Vydrov, G. E. Scuseria, L. A. Constantin, X. Zhou, and K. Burke, Phys. Rev. Lett. **100**, 136406 (2008).
[33] S. Grimme, J. Comput. Chem. **27**, 1787 (2006).
[34] CP2K DevelopersGroup, http://www.cp2k.org.
[35] T. Lu and F. Chen, J. Comput. Chem. **33**, 580 (2012).
[36] T. Lu and Q. Chen, J. Comput. Chem. **43**, 539 (2022).
[37] W. Humphrey, A. Dalke, and K. Schulten, J. Mol. Graph. Model. **14**, 33 (1996).
[38] L. Zhang, J. Ren, Y. He, and X. Chen, Appl. Surf. Sci. **622**, 156947 (2023).
[39] B. Assfour and G. Seifert, Microporous Mesoporous Mater. **133**, 59 (2010).
[40] S. L. Mayo and B. D. Olafson, J. Phys. Chem. C **94**, 8897 (1990).
[41] F. Zhang, Q. Wu, X. Bi, W. Chen, X. Huang, L. Bi, Y. Xu, G. Yan, H. Zhao, J. Hu, Y. Wang, and Z. Yang, Surf. Interfaces **34**, 102395 (2022).
[42] Y. Han, T. Hu, X. Liu, S. Jia, H. Liu, J. Hu, G. Zhang, L. Yang, G. Hong, and Y. T. Chen, Phys. Chem. Chem. Phys. **25**, 11613 (2023).
[43] F. F. Monteiro, W. F. Giozza, R. T. S. Junior, P. H. de Oliveira Neto, L. A. R. Junior, and M. L. P. Junior, J. Mol. Model. **29**, 215 (2023).
[44] See Supplemental Material at http://link.aps.org/supplemental/10.1103/PhysRevMaterials.8.075401 for the optimized structures and charge density difference of Li-decorated C-doped BN configurations; PDOS and Bader charge of BNC_{NN} monolayer and Li-decorated BNC_{NN} monolayer; structure and adsorption energy of single hydrogen molecule directly adsorbed on BNC_{NN}; more calculations of Li-decorated BNC_{NN} with 24 H_2 (including PDOS, charge density difference, Bader charge, AIMD simulations at 300 and 600 K); interaction between Li and BNC_{NN} (or H_2 molecules) by IGMH method; the Morse potential force field parameters; comparison of hydrogen storage performance of different Li-modified B-N-C 2D materials. The Supplemental Material also contains Refs. [23–25,51–55].
[45] L. Bi, J. Yin, X. Huang, Y. Wang, and Z. Yang, Int. J. Hydrogen Energy **44**, 15183 (2019).
[46] Y. Zhang, P. Liu, X. Zhu, and Z. Liu, Int. J. Hydrogen Energy **46**, 32936 (2021).
[47] M. Jiang, J. Xu, P. Munroe, and Z.-H. Xie, Appl. Surf. Sci. **618**, 156707 (2023).
[48] L. Tang, S. Shi, C. Yao, S. Zhang, Y. Liu, Z. Duan, J. Jiang, and D. Chen, Appl. Surf. Sci. **648**, 159078 (2024).
[49] Q. Yin, G. Bi, R. Wang, Z. Zhao, and K. Ma, Int. J. Hydrogen Energy **48**, 26288 (2023).
[50] L. Zhang, J. Ren, J. Cheng, and X. Chen, J. Energy Storage **80**, 110217 (2024).
[51] B. Chettri, P. K. Patra, N. N. Hieu, and D. P. Rai, Surf. Interfaces **24**, 101043 (2021).
[52] N. Khossossi, Y. Benhouria, S. R. Naqvi, P. K. Panda, I. Essaoudi, A. Ainane, and R. Ahuja, Sustain. Energy Fuels **4**, 4538 (2020).
[53] Y. Song, H. S. Chen, Y. Zhang, and Y. H. Yin, Environ. Prog. Sustainable Energy **40**, e13623 (2021).
[54] Z. Yang and J. Ni, Appl. Phys. Lett. **100**, 183109 (2012).
[55] S. P. Kaur, T. Hussain, T. Kaewmaraya, and T. J. D. Kumar, Int. J. Hydrogen Energy **48**, 26301 (2023).
[56] T.-C. Lim, Z. Naturforsch. A **58**, 615 (2003).